J Pharmacol Sci **114**, 390 – 398 (2010)

Journal of Pharmacological Sciences

Full Paper

Methylglyoxal Augments Angiotensin II–Induced Contraction in Rat Isolated Carotid Artery

Masashi Mukohda[1], Hideyuki Yamawaki[1,*], Muneyoshi Okada[1], and Yukio Hara[1]

[1]*Laboratory of Veterinary Pharmacology, School of Veterinary Medicine, Kitasato University, Aomori 034-8628, Japan*

Received August 9, 2010; Accepted September 28, 2010

Abstract. Methylglyoxal (MGO), a metabolite of glucose, accumulates in vascular tissues of a hypertensive animal. In the present study, we examined the effect of MGO on angiotensin (Ang) II–induced contraction of rat carotid artery. Treatment of carotid artery with MGO (420 μM, 30 min) significantly augmented Ang II (0.1 to 30 nM)–induced concentration-dependent contraction. The effect was abolished by the removal of endothelium. BQ-123 (1, 5 μM), an endothelin A–receptor blocker, had no effect on the MGO-induced enhancement of Ang II–induced contraction. AL8810 (1 μM), a prostaglandin $F_{2\alpha}$–receptor blocker, or SQ29548 (1 μM), a thromboxane A_2–receptor blocker, was also ineffective. However, tempol (10 μM), a superoxide scavenger, and catalase (5000 U/mL), which metabolizes hydrogen peroxide to water, significantly prevented the effect of MGO. Combined MGO and Ang II treatment increased reactive oxygen species (ROS) production. Apocynin (10 μM) or gp91ds-tat (3 μM), an inhibitor of nicotinamide adenine dinucleotide phosphate (NADPH) oxidase, significantly prevented the effect of MGO. Gp91ds-tat or an Ang II type 1–receptor (AT1R) blocker, losartan (10 μM), prevented the MGO-mediated increased ROS production. The present study revealed that MGO augments Ang II–induced contraction by increasing AT1R-mediated NADPH oxidase–derived superoxide and hydrogen peroxide production in endothelium of rat carotid artery.

Keywords: glucose metabolite, vascular endothelium, angiotensin, reactive oxygen species, smooth muscle contractility

Introduction

Methylglyoxal (MGO) is a reactive alpha-dicarbonyl compound that originates from various biochemical pathways. MGO is mainly produced in the process of glycolysis from dihydroxyacetone phosphate as a by-product during the formation of glyceraldehyde 3-phosphates in vascular smooth muscle cells (VSMCs) (1) and endothelial cells (ECs) (2). MGO binds to and modifies arginine, lysine, and cysteine residues in proteins, which leads to the non-enzymatic formation of a variety of advanced glycation end-products (AGEs) (3) including argpyrimidine (4) and N^{ε}-(carboxyethyl)lysine (5).

Angiotensin (Ang) II is one of the physiologically active peptides and induces vascular smooth muscle contraction via Ang II type 1 receptor (AT1R) (6). Moreover, Ang II stimulates reactive oxygen species (ROS) production via AT1R-activated nicotinamide adenine dinucleotide phosphate (NADPH) oxidase in VSMCs and ECs (7, 8). Ang II–derived ROS contributes to the development of hypertension and atherosclerosis (9, 10).

Several reports showed that the concentration of MGO is significantly increased in plasma from diabetic patients (11) and in tissues from diabetic animals (12). Increased plasma MGO-derived AGEs level seems to be associated with diabetic vascular complications such as diabetic retinopathy (13) and nephropathy (14). In addition, it was reported that MGO accumulated in the aorta of spontaneous hypertensive rats (SHR) with aging and that the increased MGO level in aorta was associated with increased blood pressure in SHR (15). It was demonstrated that administration of MGO by drinking water not only increased blood pressure in Wistar-Kyoto rats (16) but also induced insulin resistance and salt-sensitive hypertension in Sprague–Dawley rats (17). Therefore we hypothesized that MGO could directly affect vascular

*Corresponding author. yamawaki@vmas.kitasato-u.ac.jp
Published online in J-STAGE on November 9, 2010 (in advance)
doi: 10.1254/jphs.10206FP

reactivity. In fact, we have previously demonstrated that acute treatment of endothelium-denuded rat aorta and mesenteric artery with MGO inhibits noradrenaline (NA)-induced contraction (18). Moreover, we showed that treatment of rat aorta with MGO had no effect on acetylcholine (ACh)-induced endothelium-dependent relaxation, but significantly increased sodium nitroprusside (SNP)-induced endothelium-independent relaxation (19). However, it remains to be clarified whether MGO could also affect vascular reactivity in isolated blood vessels other than rat aorta and mesenteric artery. Furthermore, the effect of MGO on contraction induced by contractile agonists other than NA including Ang II is not determined yet. Therefore, in the present study, we examined effects of MGO on Ang II–induced contraction of rat isolated carotid artery.

Materials and Methods

Tissue preparation

Male Wistar rats (0.2 – 0.4 kg, 5 – 10-week-old) were anesthetized with urethane (1.5 g/kg, i.p.) and euthanized by exsanguination. The common carotid artery was isolated. After removal of fat and adventitia, the carotid artery was cut into rings for the measurement of isometric tension (18, 19). Endothelium was removed by rubbing the intimal surface with the flat face of a pair of forceps, and it was confirmed by the lack of relaxation induced by ACh (1 – 10 μM). Animal care and treatment were conducted in conformity with institutional guidelines of The Kitasato University.

Measurement of isometric tension

The arterial preparations were placed in normal physiological salt solution (PSS), which contained 136.9 mM NaCl, 5.4 mM KCl, 1.5 mM $CaCl_2$, 1.0 mM $MgCl_2$, 23.8 mM $NaHCO_3$, 5.5 mM glucose, and 0.001 mM EDTA. The high-K^+ (72.7 mM) solution was prepared by replacing NaCl with equimolar KCl. These solutions were saturated with a 95% O_2 – 5% CO_2 mixture at 37°C and pH 7.4. Smooth muscle contractility was recorded isometrically with a force-displacement transducer (Nihon Kohden, Tokyo) as described previously (18, 19). The arterial preparations were equilibrated for 30 min under a resting tension of 0.5 g. The arterial preparations were then repeatedly exposed to high-K^+ solution until the responses became stable (45 min). Concentration–responses curves to Ang II (0.1 – 30 nM) and NA (1 nM – 1 μM) were obtained by the cumulative application of the agonists. The concentrations of Ang II yielding the maximal contraction differed in each vessel. For example in Fig. 1B, 10 nM Ang II induced maximal contraction in most vessels (9 of 10 vessels), whereas in some vessels, 3 or 30 nM Ang II induced maximal contraction. ACh (1 nM – 300 μM) was cumulatively applied to the arteries pre-contracted to the similar level with NA (for control: 60 nM and for MGO: 100 nM). We performed 2 sequential experiments to achieve the concentration–response curves to Ang II and NA in the identical arterial rings (1st experiment: control, 2nd experiment: MGO alone or MGO + inhibitor). It was confirmed that control sequential experiments done after 30 min without MGO showed the same contractile profile as the preceding control. Effect of MGO on ACh-induced relaxation was examined in the different arterial rings. MGO was pretreated for 30 min before the Ang II– or NA-induced contraction.

Fluorometric measurement of ROS

Levels of ROS were measured by using a ROS-sensitive dye, 2′,7′-dichlorohydrofluroscin diacetate (H_2DCFDA; Invitrogen, Carlsbad, CA, USA). The common carotid artery was cut into rings for the H_2DCFDA staining. The arterial preparations were stabilized for 30 min in normal PSS saturated with a 95% O_2 – 5% CO_2 mixture at 37°C and pH 7.4 without resting tension. After treatment with Ang II (3 nM, 5 min) in the absence or presence of MGO (420 μM, 30 min) or MGO alone, H_2DCFDA was treated for 30 min. H_2O_2 (300 μM, 15 min) and *N*-acetyl-L-cysteine (NAC; 10 mM, 30 min pretreatment before Ang II) were used as a positive and negative control, respectively. Images of the endothelial surface were obtained with the fluorescence microscope (BX-51; Olympus, Tokyo) equipped with a CCD camera (MicroPublisher 5.0 RTV; Roper Industries, Sarasota, FL, USA). Image J software was used for the quantitative analysis.

Measurement of ROS by electron spin resonance (ESR) spin trapping method

ROS production was analyzed with the use of the ESR spin trapping method by using 5-(2,2-dimethyl-1,3-propoxy cyclophosphoryl)-5-methyl-1-pyrroline *N*-oxide (CYPMPO) as a spin trapping reagent. CYPMPO was previously evaluated for spin-trapping capabilities against hydroxyl and superoxide radicals (20). The arterial preparations were stabilized in normal PSS as described above. The arterial preparation was then treated with Ang II (3 nM, 5 min) in the absence or presence of MGO (420 μM, 30 min) or with MGO alone in the presence of 10 mM CYPMPO, and the PSS was collected. X-band ESR spectra in the collected PSS were recorded using a JES-FA 100 spectrometer (JEOL, Ltd., Tokyo) (21). ESR measurements were preformed under the following conditions: modulation frequency, 9.4 GHz; field modulation, 100 kHz; modulation amplitude, 0.2 mT;

microwave power, 4 mW; center field, 335.9 mT; sweep width, 5 mT; sweep time, 2 min; and time constant, 0.03 s. All spectra were recorded in the flat cells at room temperature.

Statistical analyses

Results are expressed as the mean ± S.E.M. Statistical evaluation of the data was performed by the paired or unpaired Student's *t*-test for comparisons between two groups and by ANOVA followed by Bonferroni's test for comparisons in more than three groups. Results were considered significant when the *P* value was less than 0.05. All pD_2 values were calculated as the $-\log_{10}EC_{50}$ by sigmoid curve fitting.

Chemicals

The chemicals used were as follows: Ang II, BQ-123, EDTA, indomethacin, MGO solution, NA, NAC, and 4-hydroxy-TEMPO (tempol) (Sigma, St. Louis, MO, USA); apocynin and catalase (Calbiochem, San Diego, CA, USA); AL8810 and SQ29548 (Cayman Chemical, Ann Arbor, MI, USA); gp91ds-tat (Anaspec, Fremont, CA, USA); losartan (LKT laboratories, St. Paul, MO, USA); and ACh (Daiichi Pharmaceutical, Tokyo). Indomethacin was dissolved in DMSO (0.1%). Other drugs were dissolved in distilled water.

Results

Effect of MGO on Ang II–induced contraction of rat carotid artery

We first examined effects of pretreatment of rat carotid artery with MGO (420 μM, 30 min) on contraction induced by Ang II (0.1 – 30 nM). Treatment of endothelium-intact artery with MGO significantly augmented Ang II–induced concentration-dependent contraction (Fig. 1: A and B, n = 10, maximal contraction induced by 1 – 10 nM Ang II: 100% for the control and 122.01 ± 3.80% for MGO, $P < 0.01$). The enhanced effect was abolished by the removal of endothelium (Fig. 1C, n = 12, maximal contraction induced by 3 – 30 nM Ang II: 100% for the control and 111.49 ± 5.99% for MGO).

Effect of MGO on NA-induced contraction or ACh-induced relaxation of rat carotid artery

Next, we examined the effect of pretreatment of rat carotid artery with MGO (420 μM, 30 min) on contraction induced by NA (1 nM – 1 μM) and relaxation induced by ACh (1 nM – 300 μM). Treatment of endothe-

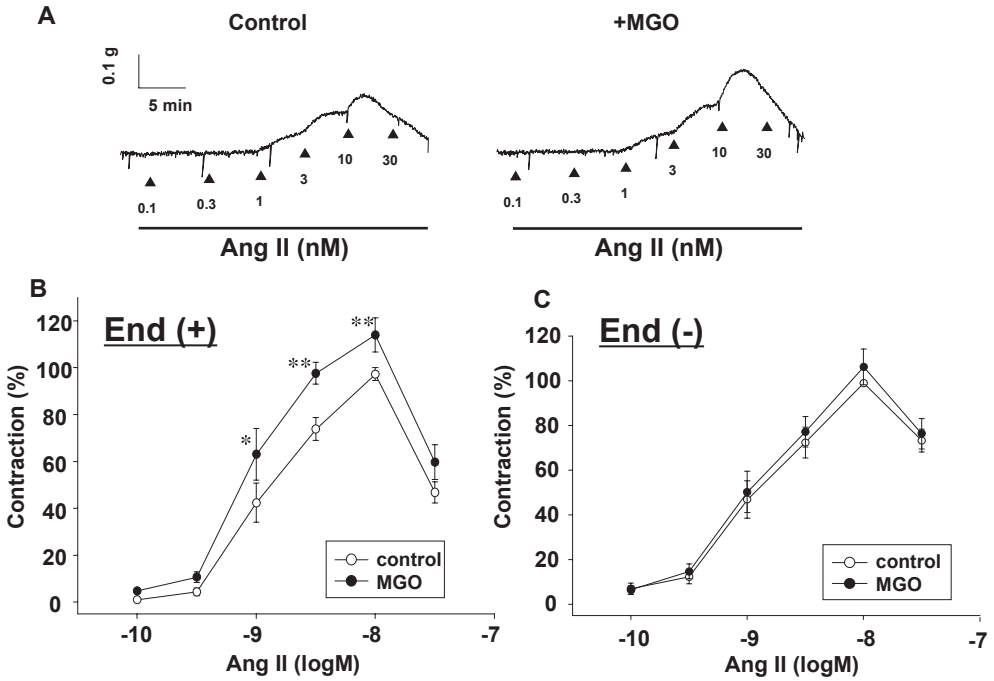

Fig. 1. Effect of pretreatment of rat carotid artery with methylglyoxal (MGO; 420 μM, 30 min) on angiotensin (Ang) II–induced concentration-dependent contraction. A: Ang II (0.1 – 30 nM) was cumulatively applied to endothelium-intact artery in the absence (control) or presence of MGO. B, C: Concentration-contraction relationships for Ang II in endothelium-intact [B, End (+)] or -denuded [C, End (−)] artery in the absence (control: open circle, n = 10 for B and n = 12 for C) or presence of MGO (MGO: closed circle, n = 10 for B and n = 12 for C). Results were expressed as the mean ± S.E.M. 100% represents Ang II (1 – 10 nM)–induced maximal contraction in control artery. *$P < 0.05$, **$P < 0.01$, control vs. MGO.

lium-intact artery with MGO had no effect on the NA-induced contraction (Fig. 2A, n = 8, pD_2; 7.84 ± 0.05 for the control and 7.82 ± 0.09 for MGO). In contrast, treatment of endothelium-denuded artery with MGO shifted the concentration–response curve for NA to the right (Fig. 2B, n = 10, pD_2: 8.03 ± 0.37 for the control vs. 7.78 ± 0.41 for MGO, $P < 0.01$). Treatment of endothelium-intact carotid artery with MGO had no effect on ACh-induced relaxation (Fig. 2C, pD_2; 6.11 ± 0.50, n = 9 for the control and 6.15 ± 0.62, n = 10 for MGO).

Effect of an endothelin-receptor blocker on MGO-induced enhancement of Ang II–induced contraction

To determine the mechanism responsible for the effect of MGO, the effect of an endothelin-receptor antagonist was examined. BQ-123 (1, 5 μM, 15 min), an endothelin A–receptor blocker, had no effect on the MGO (420 μM, 30 min)–induced enhancement of Ang II (0.1 to 30 nM)–induced contraction [Fig. 3A, maximal contraction: 100%, n = 13 for the control; 123.05 ± 4.69%, n = 5 for MGO; 124.27 ± 13.52%, n = 4 for BQ-123 (1 μM) + MGO; 125.08 ± 15.88%, n = 4 for BQ-123 (5 μM) + MGO, $P < 0.05$ between the control and MGO, BQ-123 (1 μM) + MGO, or BQ-123 (5 μM) + MGO].

Effect of prostaglandin (PG) receptor blockers on MGO-induced enhancement of Ang II–induced contraction

Next, we examined effects of PG-receptor blockers on the effect of MGO. Treatment with AL8810 (1 μM, 15 min), a $PGF_{2\alpha}$-receptor blocker, did not prevent the MGO (420 μM, 30 min)–induced enhancement of Ang II (0.1 to 30 nM)–induced contraction [Fig. 3B, maximal contraction: 100%, n = 11 for the control; 129.08 ± 15.56%, n = 6 for MGO; 120.31 ± 15.53%, n = 6 for AL8810 + MGO]. Treatment with a thromboxane A_2–receptor blocker, SQ29548 (1 μM, 15 min), was also ineffective (Fig. 3C, maximal contraction: 100%, n = 6 for the control; 160.63 ± 31.50%, n = 3 for MGO; 140.11 ± 36.67%, n = 3 for SQ29548 + MGO). We confirmed that AL8810 (n = 3) or SQ29548 (n = 2)–alone treatment had no ef-

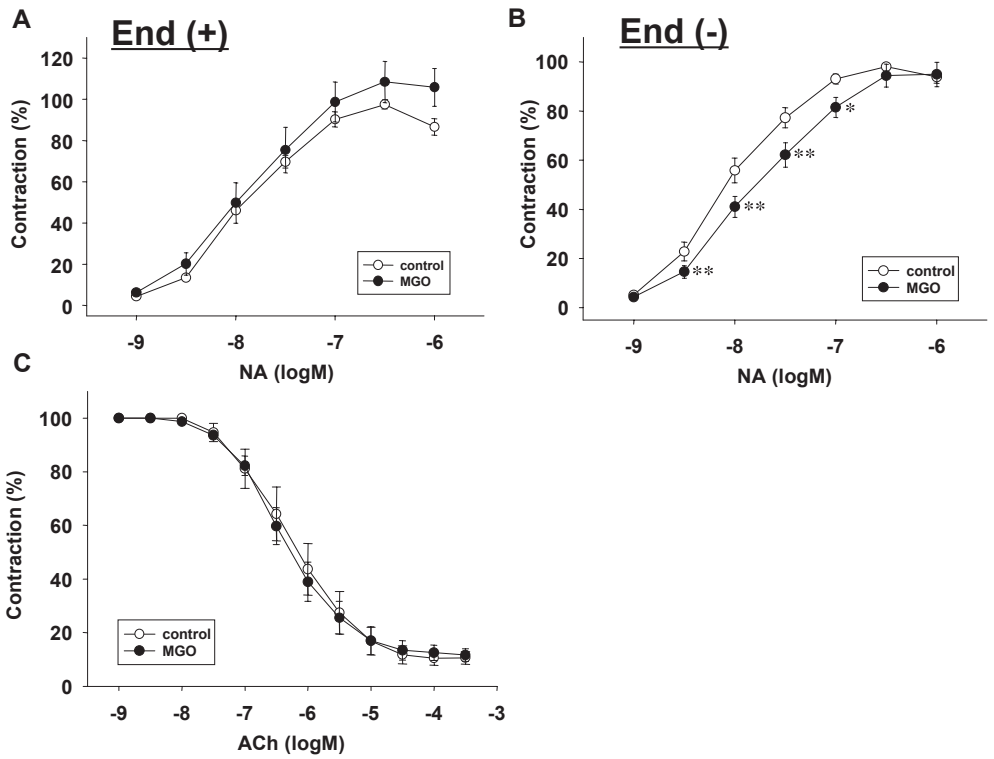

Fig. 2. Effect of MGO on noradrenaline (NA)-induced contraction or acetylcholine (ACh)-induced relaxation of rat carotid artery. Effect of pretreatment of endothelium-intact [A, End (+); control: open circle, n = 7] and -denuded [B, End (−); control: open circle, n = 10] rat carotid artery with MGO (420 μM, 30 min; MGO: closed circle, n = 7 for A and n = 10 for B) on NA (1 nM to 1 μM)–induced concentration-dependent contraction. NA was cumulatively applied, and 100% represents NA (100 nM to 1 μM)–induced maximal contraction in control artery. C: Effect of pretreatment of endothelium-intact carotid artery with MGO on relaxation induced by ACh (1 nM – 300 μM; control: open circle, n = 9 and MGO: closed circle, n = 10) on NA (for control: 60 nM and for MGO: 100 nM)–induced pre-contraction. ACh was cumulatively added after the contraction induced by NA had reached a steady state. 100% represents NA-induced pre-contraction. Results were expressed as the mean ± S.E.M. *$P < 0.05$, **$P < 0.01$, control vs. MGO.

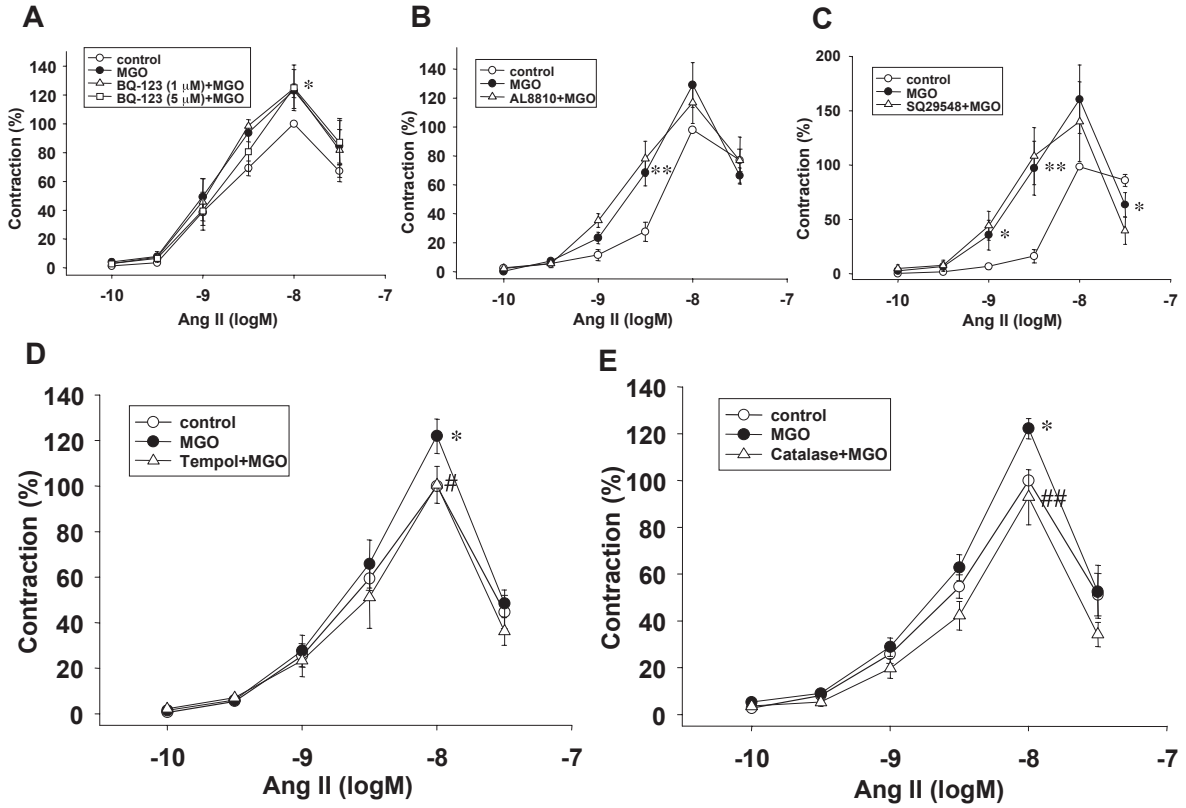

Fig. 3. Concentration–contraction relationships for Ang II in endothelium-intact rat carotid artery in the absence (control: open circle, n = 13 for A, n = 11 for B, n = 6 for C, n = 9 for D, and n = 8 for E) or presence of MGO (420 μM, 30 min) pretreated without (MGO: closed circle, n = 5 for A, n = 6 for B, n = 3 for C, n = 9 for D, and n = 8 for E) or with BQ-123 (A: 1 μM, 15 min, open triangle, n = 4; 5 μM, open square, n = 4), AL8810 (B: 1 μM, 15 min, open triangle, n = 6), SQ29548 (C: 1 μM, 15 min, open triangle, n = 3), tempol (D: 10 μM, 15 min, open triangle, n = 8), or catalase (E: 5000 U/mL, 15 min, open triangle, n = 7). Results were expressed as the mean ± S.E.M. 100% represents Ang II (10 to 30 nM)–induced maximal contraction in control artery. *$P < 0.05$, **$P < 0.01$, control vs. MGO; $^{\#}P < 0.05$, MGO vs. tempol + MGO; $^{\#\#}P < 0.01$, MGO vs. catalase + MGO.

fects on the Ang II–induced contraction.

Effect of anti-oxidant drugs on MGO-induced enhancement of Ang II–induced contraction

To further explore mechanisms, we used anti-oxidant drugs. A superoxide scavenger, tempol (10 μM, 15 min), significantly prevented the MGO (420 μM, 30 min)–induced enhancement of Ang II (0.1 to 30 nM)–induced contraction (Fig. 3D, maximal contraction: 100%, n = 9 for the control; 121.99 ± 7.54%, n = 9 for MGO; 100.64 ± 8.08%, n = 8 for tempol + MGO, $P < 0.05$ between the control and MGO, $P < 0.05$ between MGO and tempol + MGO). Treatment with catalase (5000 U/mL, 15 min), which metabolizes H_2O_2 to H_2O significantly inhibited the effect of MGO (Fig. 3E, maximal contraction: 100%, n = 8 for the control; 122.27 ± 4.36%, n = 8 for MGO; 92.96 ± 11.78%, n = 7 for catalase + MGO, $P < 0.05$ between the control and MGO, $P < 0.01$ between MGO and catalase + MGO). We confirmed that exogenously applied H_2O_2 (100 μM) augmented the Ang II (10 nM)–induced contraction (n = 7, 115.1 ± 2.8% relative to Ang II alone–induced contraction, data not shown).

Effect of MGO on Ang II–induced ROS production

We next examined effects of MGO on Ang II–induced ROS production by using a ROS-sensitive dye, H_2DCFDA. Treatment of endothelium-intact carotid artery with Ang II (3 nM, 5 min) alone slightly induced ROS production in the endothelial surface as shown in Fig. 4, A and B (n = 4, 1.81 ± 0.76-fold relative to the control). MGO (420 μM, 30 min)–alone treatment also produced a weak ROS (n = 4, 2.16 ± 0.59-fold relative to the control). Combined MGO and Ang II treatment significantly enhanced the ROS production (n = 4, 3.76 ± 0.62-fold relative to the control, $P < 0.05$ vs. control). It was confirmed that this enhanced effect of MGO on ROS production was mediated via AT1R since an AT1R blocker, losartan, significantly prevented it (n = 4, Ang II + MGO; 9.31 ± 2.57-fold relative to the

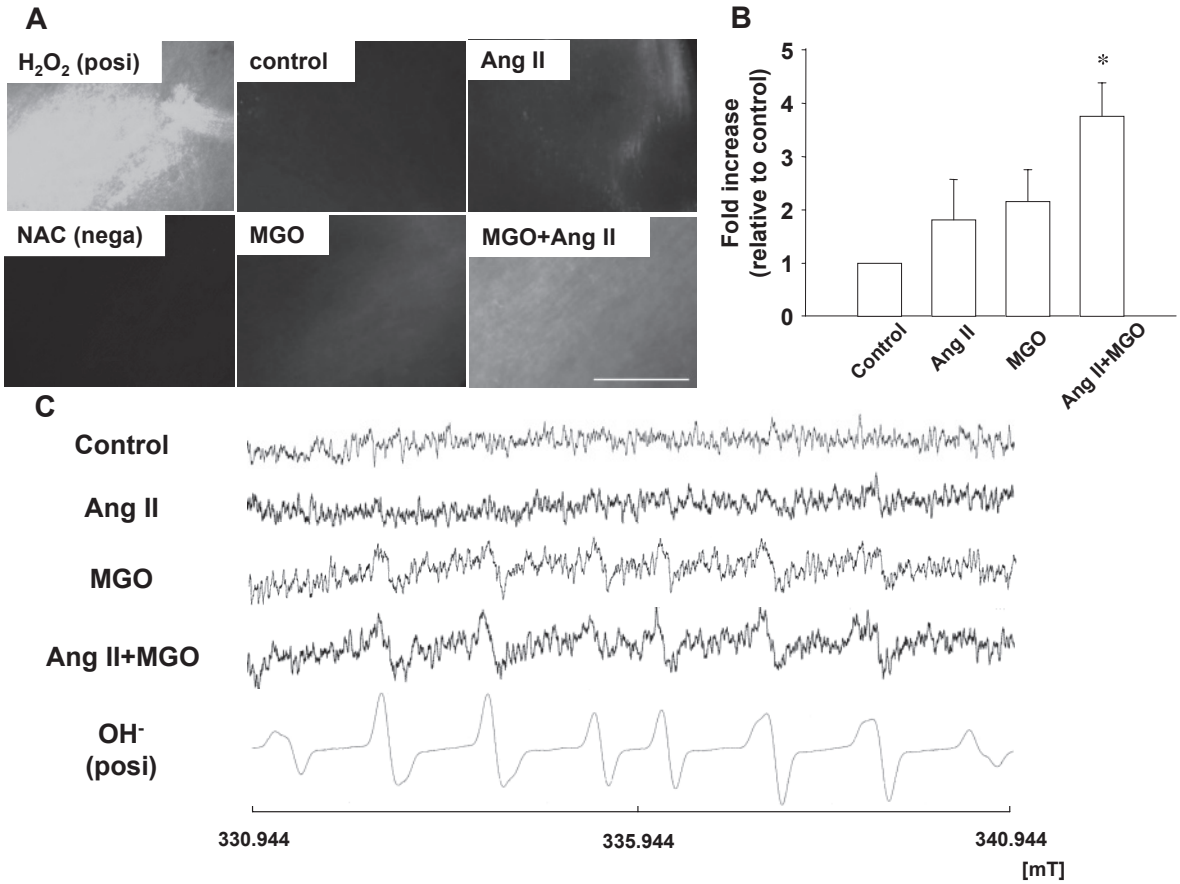

Fig. 4. Effect of MGO on Ang II–induced reactive oxygen species (ROS) production. A: ROS production in endothelium-intact rat carotid artery was determined by a fluorescence staining using H_2DCFDA. After treatment with Ang II (3 nM, 5 min) in the absence or presence of MGO (420 μM, 30 min pretreatment) or with MGO alone, carotid arteries were loaded with H_2DCFDA (10 μM, 20 min). H_2O_2 (300 μM, 15 min) and NAC (10 mM, 30 min pretreatment before Ang II) were used as a positive and negative control, respectively. Images of the endothelial surface were obtained with the fluorescence microscope. Scale bar: 50 μm. B: Fluorescent intensity was measured using Image J software and is shown as fold increase relative to the control (n = 4). *$P < 0.05$, control vs. MGO. C: ESR spectra of CYPMPO-OH adduct obtained from the 10 mM CYPMPO–containing PSS collected after treatment of endothelium-intact rat carotid artery with Ang II (10 nM, 5 min) in the absence or presence of MGO (420 μM, 30 min) or with MGO alone. The positive control (CYPMPO-OH adduct) was obtained by reacting H_2O_2 (600 μM) and $FeSO_4$ (600 μM).

control vs. losartan + Ang II + MGO; 2.46 ± 0.57-fold relative to the control, $P < 0.05$). We further analyzed the effect of MGO on Ang II–induced ROS production with the use of the ESR spin trapping method by using CYPMPO (10 mM). As shown in Fig. 4C, the CYPMPO-OH adduct signal in the PSS collected after incubating arterial samples was detected. Treatment of endothelium-intact carotid artery with Ang II (10 nM, 5 min) alone induced an undetectable level of CYPMPO-OH adduct in the PSS. In contrast, MGO (420 μM, 30 min)–alone treatment induced a detectable level of CYPMPO-OH adduct, and combined MGO and Ang II treatment enhanced it. The signal of the positive control (CYPMPO-OH adduct) was induced by reacting H_2O_2 (600 μM) and $FeSO_4$ (600 μM). It should be noted that we did not detect the CYPMPO-superoxide adduct in contrast to the results of tempol as described above (Fig. 3D). We assume that this is due to the catabolism of superoxide to hydroxyl radical.

Effect of NADPH oxidase inhibitors on MGO-induced enhancement of Ang II–induced contraction

We finally analyzed mechanism by which MGO enhanced Ang II–induced ROS production. An NAPDH oxidase inhibitor, apocynin (10 μM, 15 min), prevented the MGO (420 μM, 30 min)–induced enhancement of Ang II (0.1 to 30 nM)–induced contraction (Fig. 5A, n = 14, maximal contraction: 100% for the control; 117.30 ± 3.73% for MGO; 99.49 ± 6.72% for apocynin + MGO, $P < 0.05$ between the control and MGO,

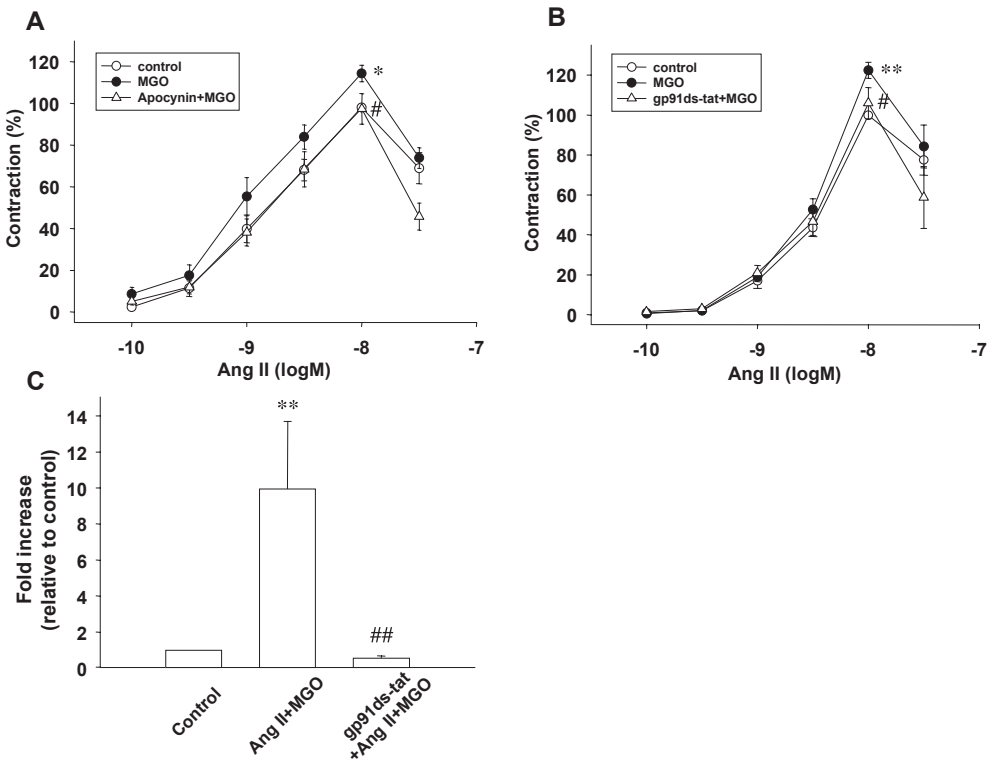

Fig. 5. Effect of NADPH oxidase inhibitors on MGO-induced enhancement of Ang II–induced contraction and ROS production. A, B: Concentration–contraction relationships for Ang II in endothelium-intact rat carotid artery in the absence (control: open circle, n = 14 for A, n = 11 for B) or presence of MGO (420 μM, 30 min) pretreated without (MGO: closed circle; n = 14 for A, n = 6 for B) or with apocynin (A, 10 μM, 15 min, open triangle, n = 14) or gp91ds-tat (B, 3 μM, 15 min, open triangle, n = 5). Results were expressed as the mean ± S.E.M. 100% represents Ang II (10 to 30 nM)–induced contraction in control artery. C: Effect of an NADPH oxidase inhibitor on MGO-induced enhancement of ROS production. ROS production in endothelium-intact rat carotid artery was fluorometrically determined. After treatment with combined Ang II (3 nM, 5 min) and MGO (420 μM, 30 min) in the absence or presence of gp91ds-tat (3 μM, 15 min), carotid arteries were loaded with H_2DCFDA (10 μM, 20 min). Fluorescent intensity of the endothelial surface was measured using Image J software and is shown as fold increase relative to the control (n = 4). *$P < 0.05$, control vs. MGO; **$P < 0.01$, control vs. MGO or Ang II + MGO; $^{\#}P < 0.05$, MGO vs. apocynin + MGO or gp91ds-tat + MGO; $^{\#\#}P < 0.01$, Ang II + MGO vs. gp91ds-tat + Ang II + MGO.

$P < 0.05$ between MGO and apocynin + MGO). Treatment with another NADPH oxidase inhibitor, gp91ds-tat (3 μM, 15 min), significantly inhibited the effect of MGO (Fig. 5B, maximal contraction: 100%, n = 11 for the control; 122.43 ± 4.01%, n = 6 for MGO; 105.92 ± 7.80%, n = 5 for gp91ds-tat + MGO, $P < 0.01$ between the control and MGO, $P < 0.05$ between MGO and gp91ds-tat + MGO). We further examined effects of the NADPH oxidase inhibitor on ROS production. Gp91ds-tat (3 μM, 15 min) completely prevented the combined Ang II and MGO–induced ROS production (Fig. 5C, n = 4, Ang II + MGO; 9.96 ± 3.75-fold relative to the control vs. gp91ds-tat + Ang II + MGO; 0.56 ± 0.11-fold relative to the control, $P < 0.01$). Gp91ds-tat alone had no effect on the basal ROS level (n = 4, 1.11 ± 0.29-fold relative to the control).

Discussion

The major finding of the present study is that treatment of endothelium-intact rat carotid artery with MGO augmented the Ang II–induced contraction (Fig. 6). The effect of MGO is dependent on endothelium, but independent of the production of endothelin or contractile PG, which is a kind of endothelium-derived contracting factor. We have determined that MGO-induced enhancement of Ang II–induced contraction is mediated via increasing ROS production, including superoxide and hydrogen peroxide. Finally, it was demonstrated that MGO-mediated increased ROS production is due to enhancing AT1R-mediated NADPH oxidase activation in the endothelium of carotid artery. Here, we clarified the novel effects of MGO on contractility of rat carotid artery.

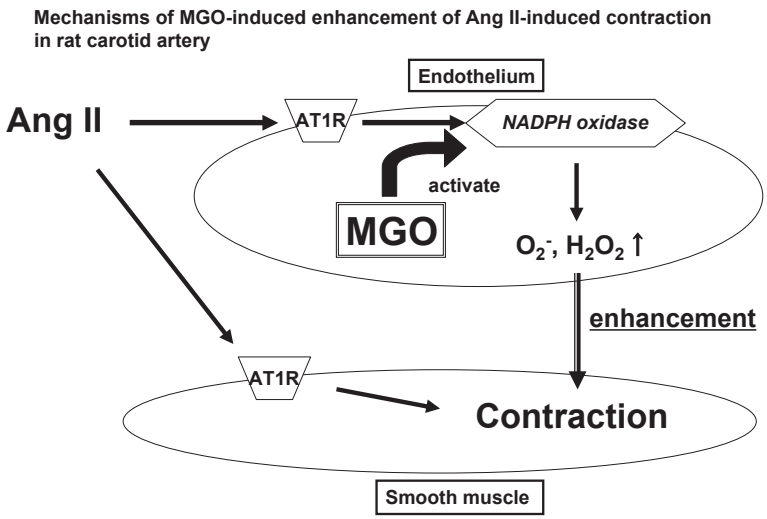

Fig. 6. Summary of the results. MGO augmented Ang II–induced contraction via increased Ang II type 1 receptor (AT1R)–mediated NADPH oxidase–derived superoxide and hydrogen peroxide production in endothelium of rat carotid artery.

In the previous studies, we demonstrated that acute treatment with MGO rather inhibited the NA-induced contraction in endothelium-denuded rat aorta and mesenteric artery (18). It was also demonstrated in rat aorta that MGO had no effect on the ACh-induced endothelium-dependent relaxation (19). In the present study, we confirmed that MGO significantly inhibited the NA-induced contraction in endothelium-denuded but not -intact rat carotid artery. It was further confirmed in rat carotid artery that MGO had no effects on the ACh-induced endothelium-dependent relaxation. These results collectively indicate that effects of MGO on vascular reactivity are different depending on the types of contractile agonists.

We found that MGO augmented the Ang II–induced contraction via increased NADPH oxidase–mediated superoxide and hydrogen peroxide production in the endothelium of rat carotid artery. It is well known that NADPH oxidase is a major source of ROS in vascular tissues (22). NADPH oxidase consists of 6 subunits; the membrane-bound $gp91^{phox}$ and $p22^{phox}$, the cytoplasmic complex $p67^{phox}$, $p40^{phox}$, and $p47^{phox}$, and the small GTPase Rac (23). It was reported that NADPH oxidase activation is mediated in part via phosphorylation of $p40^{phox}$ or $p47^{phox}$ and that protein kinase C could mediate the $p47^{phox}$ phosphorylation (24, 25). We have previously demonstrated that MGO induced phosphorylation of JNK and p38 in cultured vascular ECs (26). Although it remains to be clarified how NADPH oxidase activity is enhanced by MGO, such phosphorylation-dependent mechanisms might be applicable. Further biochemical studies might help to clarify the mechanisms through which MGO enhances NADPH oxidase activity in endothelium of rat carotid artery.

We showed that treatment of endothelium-intact rat carotid artery with MGO enhanced the Ang II–induced contraction by increasing superoxide and hydrogen peroxide production. Superoxide and hydrogen peroxide are kinds of ROS produced from endothelial nitric oxide (NO) synthase, NADPH oxidase, xanthine oxidase, and the mitochondrial respiratory chain as the major sources (27). It was previously demonstrated that endothelium-derived ROS mediates contraction by elevating the intracellular Ca^{2+} concentration in pulmonary arterial smooth muscle (28), by activating thromboxane A_2 (TP) receptor in aorta from SHR (29), and by inhibiting endothelium-derived relaxing factor (NO) in rat aorta (30). It seems unlikely in the present study that the TP receptor is responsible for the increased contraction, since the TP-receptor blocker SQ29548 did not affect the MGO-induced enhancement of Ang II–induced contraction. Nonetheless, it might be possible in rat carotid artery that MGO-induced increase of Ang II–induced superoxide or hydrogen peroxide could mediate vasoconstriction by the other mechanisms described above.

In summary, we for the first time demonstrated that MGO has an augmenting effect on Ang II–induced contraction of rat carotid artery. The effect was mediated via increased NADPH oxidase–mediated superoxide and hydrogen peroxide production in endothelium. Further studies including determining the chronic effect of MGO might contribute to provide mechanistic insights into roles of MGO in the development of hypertensive vascular diseases.

Acknowledgments

We are grateful to Dr. Shunji Ueno for excellent technical assistance with the ESR method and to Dr. Masato Kamibayashi for providing CYPMPO. This study was supported in part by Grants for Scientific Research from the Kitasato University, School of Veterinary

Medicine and from the Japan Society for the Promotion of Science (JSPS). Dr. Masashi Mukohda, DVM is a Research Fellow of the JSPS.

References

1 Wu L. Is methylglyoxal a causative factor for hypertension development? Can J Physiol Pharmacol. 2006;84:129–139.
2 Schalkwijk CG, Van Bezu J, Van Der Schors RC, Uchida K, Stehouwer CD, Van Hinsbergh VW. Heat-shock protein 27 is a major methylglyoxal-modified protein in endothelial cells. FEBS Lett. 2006;580:1565–1570.
3 Yim HS, Kang SO, Hah YC, Chock PB, Yim MB. Free radicals generated during the glycation reaction of amino acids by methylglyoxal. A model study of protein-cross-linked free radicals. J Biol Chem. 1995;270:28228–28233.
4 Oya T, Hattori N, Mizuno Y, Miyata S, Maeda S, Osawa T, et al. Methylglyoxal modification of protein. Chemical and immunochemical characterization of methylglyoxal-arginine adducts. J Biol Chem. 1999;274:18492–18502.
5 Ahmed MU, Brinkmann Frye E, Degenhardt TP, Thorpe SR, Baynes JW. N-epsilon-(carboxyethyl)lysine, a product of the chemical modification of proteins by methylglyoxal, increases with age in human lens proteins. Biochem J. 1997;324:565–570.
6 Mugabe BE, Yaghini FA, Song CY, Buharalioglu CK, Waters CM, Malik KU. Angiotensin II-induced migration of vascular smooth muscle cells is mediated by p38 mitogen-activated protein kinase-activated c-Src through spleen tyrosine kinase and epidermal growth factor receptor transactivation. J Pharmacol Exp Ther. 2010;332:116–124.
7 Rush JW, Aultman CD. Vascular biology of angiotensin and the impact of physical activity. Appl Physiol Nutr Metab. 2008;33:162–172.
8 Gao L, Mann GE. Vascular NAD(P)H oxidase activation in diabetes: a double-edged sword in redox signalling. Cardiovasc Res. 2009;82:9–20.
9 Weiss D, Sorescu D, Taylor WR. Angiotensin II and atherosclerosis. Am J Cardiol. 2001;87:25C–32C.
10 Kobori H, Nangaku M, Navar LG, Nishiyama A. The intrarenal renin-angiotensin system: from physiology to the pathobiology of hypertension and kidney disease. Pharmacol Rev. 2007;59:251–287.
11 Lapolla A, Flamini R, Dalla Vedova A, Senesi A, Reitano R, Fedele D, et al. Glyoxal and methylglyoxal levels in diabetic patients: quantitative determination by a new GC/MS method. Clin Chem Lab Med. 2003;41:1166–1173.
12 Phillips SA, Mirrlees D, Thornalley PJ. Modification of the glyoxalase system in streptozotocin-induced diabetic rats. Effect of the aldose reductase inhibitor Statil. Biochem Pharmacol. 1993;46:805–811.
13 Fosmark DS, Torjesen PA, Kilhovd BK, Berg TJ, Sandvik L, Hanssen KF, et al. Increased serum levels of the specific advanced glycation end product methylglyoxal-derived hydroimidazolone are associated with retinopathy in patients with type 2 diabetes mellitus. Metabolism. 2006;55:232–236.
14 Mostafa AA, Randell EW, Vasdev SC, Gill VD, Han Y, Gadag V, et al. Plasma protein advanced glycation end products, carboxymethyl cysteine, and carboxyethyl cysteine, are elevated and related to nephropathy in patients with diabetes. Mol Cell Biochem. 2007;302:35–42.
15 Wang X, Desai K, Chang T, Wu L. Vascular methylglyoxal metabolism and the development of hypertension. J Hypertens. 2005;23:1565–1573.
16 Vasdev S, Ford CA, Longerich L, Parai S, Gadag V, Wadhawan S. Aldehyde induced hypertension in rats: prevention by N-acetyl cysteine. Artery. 1998;23:10–36.
17 Guo Q, Mori T, Jiang Y, Hu C, Osaki Y, Yoneki Y, et al. Methylglyoxal contributes to the development of insulin resistance and salt sensitivity in Sprague-Dawley rats. J Hypertens. 2009;27:1664–1671.
18 Mukohda M, Yamawaki H, Nomura H, Okada M, Hara Y. Methylglyoxal inhibits smooth muscle contraction in isolated blood vessels. J Pharmacol Sci. 2009;109:305–310.
19 Mukohda M, Yamawaki H, Okada M, Hara Y. Methylglyoxal enhances sodium nitroprusside-induced relaxation in rat aorta. J Pharmacol Sci. 2010;112:176–183.
20 Ogura A, Oowada S, Kon Y, Hirayama A, Yasui H, Meike S, et al. Redox regulation in radiation-induced cytochrome c release from mitochondria of human lung carcinoma A549 cells. Cancer Lett. 2009;277:64–71.
21 Ueno S, Kashimoto T, Susa N, Wada K, Ito N, Takeda-Homma S, et al. Estimation of hydroxyl radical generation by salicylate hydroxylation method in multiple organs of mice exposed to whole-body X-ray irradiation. Free Radic Res. 2006;40:944–951.
22 Lassegue B, Griendling KK. NADPH oxidases: functions and pathologies in the vasculature. Arterioscler Thromb Vasc Biol. 2010;30:653–661.
23 El-Benna J, Dang PM, Gougerot-Pocidalo MA. Priming of the neutrophil NADPH oxidase activation: role of p47phox phosphorylation and NOX2 mobilization to the plasma membrane. Semin Immunopathol. 2008;30:279–289.
24 Babior BM. NADPH oxidase: an update. Blood. 1999;93:1464–1476.
25 Williams HC, Griendling KK. NADPH oxidase inhibitors: new antihypertensive agents? J Cardiovasc Pharmacol. 2007;50:9–16.
26 Yamawaki H, Saito K, Okada M, Hara Y. Methylglyoxal mediates vascular inflammation via JNK and p38 in human endothelial cells. Am J Physiol Cell Physiol. 2008;295:C1510–C1517.
27 Manrique C, Lastra G, Gardner M, Sowers JR. The renin angiotensin aldosterone system in hypertension: roles of insulin resistance and oxidative stress. Med Clin North Am. 2009;93:569–582.
28 Wang YX, Zheng YM. ROS-dependent signaling mechanisms for hypoxic Ca(2+) responses in pulmonary artery myocytes. Antioxid Redox Signal. 2010;12:611–623.
29 Yang D, Feletou M, Boulanger CM, Wu HF, Levens N, Zhang JN, et al. Oxygen-derived free radicals mediate endothelium-dependent contractions to acetylcholine in aortas from spontaneously hypertensive rats. Br J Pharmacol. 2002;136:104–110.
30 Srivastava P, Hegde LG, Patnaik GK, Dikshit M. Role of endothelial-derived reactive oxygen species and nitric oxide in norepinephrine-induced rat aortic ring contractions. Pharmacol Res. 1998;38:265–274.